Research Article | Vol. 25, No. 16 | 7 Aug 2017 | OPTICS EXPRESS 19195
Optics EXPRESS

Acceleration of sub-relativistic electrons with an evanescent optical wave at a planar interface

M. Kozák,[1,*] P. Beck,[1] H. Deng,[2] J. McNeur,[1] N. Schönenberger,[1] C. Gaida,[3] F. Stutzki,[3] M. Gebhardt,[3,4] J. Limpert,[3,4] A. Ruehl,[5] I. Hartl,[5] O. Solgaard,[2] J. S. Harris,[2,6] R. L. Byer,[6] and P. Hommelhoff[1,7]

[1]*Department of Physics, Friedrich-Alexander-Universität Erlangen-Nürnberg (FAU), Staudtstrasse 1, 91058 Erlangen, Germany*
[2]*Department of Electrical Engineering, Stanford University, Stanford, California 94305, USA*
[3]*Institute of Applied Physics, Friedrich-Schiller-Universität Jena, Albert-Einstein-Strasse 15, 07745, Jena, Germany*
[4]*Helmholtz-Institute Jena, Fröbelstieg 3, 07743 Jena, Germany*
[5]*Deutsches Elektronen-Synchrotron DESY, D-22607 Hamburg, Germany*
[6]*Department of Applied Physics, Stanford University, Stanford, California 94305, USA*
[7]*Max Planck Institute for the Science of Light, Staudtstrasse 2, 91058 Erlangen, Germany*
[*]*martin.kozak@fau.de*

Abstract: We report on a theoretical and experimental study of the energy transfer between an optical evanescent wave, propagating in vacuum along the planar boundary of a dielectric material, and a beam of sub-relativistic electrons. The evanescent wave is excited via total internal reflection in the dielectric by an infrared (λ = 2 μm) femtosecond laser pulse. By matching the electron propagation velocity to the phase velocity of the evanescent wave, energy modulation of the electron beam is achieved. A maximum energy gain of 800 eV is observed, corresponding to the absorption of more than 1000 photons by one electron. The maximum observed acceleration gradient is 19 ± 2 MeV/m. The striking advantage of this scheme is that a structuring of the acceleration element's surface is not required, enabling the use of materials with high laser damage thresholds that are difficult to nano-structure, such as SiC, Al_2O_3 or CaF_2.

OCIS codes: (350.4990) Particles; (320.7120) Ultrafast phenomena; (290.5850) Scattering, particles; (240.6690) Surface waves.

References and links

1. T. Tajima and J. M. Dawson, "Laser Electron Accelerator," Phys. Rev. Lett. **43**(4), 267–270 (1979).
2. C. Joshi, W. B. Mori, T. Katsouleas, J. M. Dawson, J. M. Kindel, and D. W. Forslund, "Ultrahigh gradient particle acceleration by intense laser-driven plasma density waves," Nature **311**(5986), 525–529 (1984).
3. W. P. Leemans, B. Nagler, A. J. Gonsalves, C. Tóth, K. Nakamura, C. G. R. Geddes, E. Esarey, C. B. Schroeder, and S. M. Hooker, "GeV electron beams from a centimetre-scale accelerator," Nat. Phys. **2**(10), 696–699 (2006).
4. X. Wang, R. Zgadzaj, N. Fazel, Z. Li, S. A. Yi, X. Zhang, W. Henderson, Y.-Y. Chang, R. Korzekwa, H.-E. Tsai, C.-H. Pai, H. Quevedo, G. Dyer, E. Gaul, M. Martinez, A. C. Bernstein, T. Borger, M. Spinks, M. Donovan, V. Khudik, G. Shvets, T. Ditmire, and M. C. Downer, "Quasi-monoenergetic laser-plasma acceleration of electrons to 2 GeV," Nat. Commun. **4**, 1988 (2013).
5. W. P. Leemans, A. J. Gonsalves, H.-S. Mao, K. Nakamura, C. Benedetti, C. B. Schroeder, C. Tóth, J. Daniels, D. E. Mittelberger, S. S. Bulanov, J.-L. Vay, C. G. R. Geddes, and E. Esarey, "Multi-GeV electron beams from capillary-discharge-guided subpetawatt laser pulses in the self-trapping regime," Phys. Rev. Lett. **113**(24), 245002 (2014).
6. R. Palmer, "Interaction of relativistic particles and free electromagnetic waves in the presence of a static helical magnet," J. Appl. Phys. **43**(7), 3014–3023 (1972).
7. E. D. Courant, C. Pellegrini, and W. Zakowicz, "High-energy inverse free-electron-laser accelerator," Phys. Rev. A Gen. Phys. **32**(5), 2813–2823 (1985).
8. A. Pukhov, Z.-M. Sheng, and J. Meyer-ter-Vehn, "Particle acceleration in relativistic laser channels," Phys. Plasmas **6**(7), 2847–2854 (1999).

#294562 https://doi.org/10.1364/OE.25.019195
Journal © 2017 Received 4 May 2017; revised 29 Jun 2017; accepted 30 Jun 2017; published 31 Jul 2017

Optics EXPRESS

9. E. A. Peralta, K. Soong, R. J. England, E. R. Colby, Z. Wu, B. Montazeri, C. McGuinness, J. McNeur, K. J. Leedle, D. Walz, E. B. Sozer, B. Cowan, B. Schwartz, G. Travish, and R. L. Byer, "Demonstration of electron acceleration in a laser-driven dielectric microstructure," Nature **503**(7474), 91–94 (2013).
10. J. Breuer and P. Hommelhoff, "Laser-based acceleration of nonrelativistic electrons at a dielectric structure," Phys. Rev. Lett. **111**(13), 134803 (2013).
11. R. J. England, R. J. Noble, K. Bane, D. H. Dowell, C.-K. Ng, J. E. Spencer, S. Tantawi, Z. Wu, R. L. Byer, E. Peralta, K. Soong, C.-M. Chang, B. Montazeri, S. J. Wolf, B. Cowan, J. Dawson, W. Gai, P. Hommelhoff, Y.-C. Huang, C. Jing, C. McGuinness, R. B. Palmer, B. Naranjo, J. Rosenzweig, G. Travish, A. Mizrahi, L. Schachter, C. Sears, G. R. Werner, and R. B. Yoder, "Dielectric laser accelerators," Rev. Mod. Phys. **86**(4), 1337–1389 (2014).
12. K. J. Leedle, A. Ceballos, H. Deng, O. Solgaard, R. F. Pease, R. L. Byer, and J. S. Harris, "Dielectric laser acceleration of sub-100 keV electrons with silicon dual-pillar grating structures," Opt. Lett. **40**(18), 4344–4347 (2015).
13. B. Barwick, D. J. Flannigan, and A. H. Zewail, "Photon-induced near-field electron microscopy," Nature **462**(7275), 902–906 (2009).
14. P. Baum and A. H. Zewail, "4D attosecond imaging with free electrons: Diffraction methods and potential applications," Chem. Phys. **366**(1-3), 2–8 (2009).
15. L. Piazza, T. T. A. Lummen, E. Quiñonez, Y. Murooka, B. W. Reed, B. Barwick, and F. Carbone, "Simultaneous observation of the quantization and the interference pattern of a plasmonic near-field," Nat. Commun. **6**, 6407 (2015).
16. M. Kozák, J. McNeur, K. J. Leedle, H. Deng, N. Schönenberger, A. Ruehl, I. Hartl, J. S. Harris, R. L. Byer, and P. Hommelhoff, "Optical gating and streaking of free electrons with sub-optical cycle precision," Nat. Commun. **8**, 14342 (2017).
17. M. Kozák, J. McNeur, K. J. Leedle, H. Deng, N. Schönenberger, A. Ruehl, I. Hartl, H. Hoogland, R. Holzwarth, J. S. Harris, R. L. Byer, and P. Hommelhoff, "Transverse and longitudinal characterization of electron beams using interaction with optical near-fields," Opt. Lett. **41**(15), 3435–3438 (2016).
18. F. J. García de Abajo, A. Asenjo-Garcia, and M. Kociak, "Multiphoton absorption and emission by interaction of swift electrons with evanescent light fields," Nano Lett. **10**(5), 1859–1863 (2010).
19. A. Feist, K. E. Echternkamp, J. Schauss, S. V. Yalunin, S. Schäfer, and C. Ropers, "Quantum coherent optical phase modulation in an ultrafast transmission electron microscope," Nature **521**(7551), 200–203 (2015).
20. K. E. Echternkamp, A. Feist, S. Schäfer, and C. Ropers, "Ramsey-type phase control of free-electron beams," Nat. Phys. **12**(11), 1000–1004 (2016).
21. J. D. Lawson, "Lasers and accelerators," IEEE Trans. Nucl. Sci. **26**(3), 4217–4219 (1979).
22. S. T. Park, M. Lin, and A. H. Zewail, "Photon-induced near-field electron microscopy (PINEM): theoretical and experimental," New J. Phys. **12**(12), 123028 (2010).
23. J. Breuer, J. McNeur, and P. Hommelhoff, "Dielectric laser acceleration of electrons in the vicinity of single and double grating structures—theory and simulations," J. Phys. At. Mol. Opt. Phys. **47**(23), 234004 (2014).
24. B. R. Frandsen, S. A. Glasgow, and J. B. Peatross, "Acceleration of free electrons in a symmetric evanescent wave," Laser Phys. **16**(9), 1311–1314 (2006).
25. L. Gallais, D.-B. Douti, M. Commandré, G. Batavičiūtė, E. Pupka, M. Ščiuka, L. Smalakys, V. Sirutkaitis, and A. Melninkaitis, "Wavelength dependence of femtosecond laser-induced damage threshold of optical materials," J. Appl. Phys. **117**(22), 223103 (2015).
26. E. Hecht, *Optics* (2nd ed., Addison Wesley, 1987).
27. J. Breuer, R. Graf, A. Apolonski, and P. Hommelhoff, "Dielectric laser acceleration of nonrelativistic electrons at a single fused silica grating structure: Experimental part," Phys. Rev. Spec. Top. Accel. Beams **17**(2), 021301 (2014).
28. H. H. Li, "Refractive index of silicon and germanium and its wavelength and temperature derivatives," J. Phys. Chem. Ref. Data **9**(3), 561–658 (1980).
29. Lumerical Solutions, Inc., "FDTD Solutions," https://www.lumerical.com/tcad-products/fdtd/.
30. H. A. H. Boot and R. B. R.-S. Harvie, "Charged Particles in a Non-uniform Radio-frequency Field," Nature **180**, 1187 (1957).
31. J. McNeur, M. Kozák, N. Schönenberger, K. J. Leedle, H. Deng, A. Ceballos, H. Hoogland, A. Ruehl, I. Hartl, O. Solgaard, J. S. Harris, R. L. Byer, and P. Hommelhoff, https://arXiv:1604.07684 (2016).
32. T. Plettner and R. L. Byer, "Proposed dielectric-based microstructure laser-driven undulator," Phys. Rev. Spec. Top. Accel. Beams **11**(3), 030704 (2008).
33. H. Deng, J. Jiang, Y. Miao, K. J. Leedle, H. Li, O. Solgaard, R. L. Byer, and J. S. Harris, Design of racetrack ring resonator based dielectric laser accelerators," https://arXiv:1701.08945 (2017).

1. Introduction

The study of the interaction between photons and free charged particles began shortly after the invention of the laser, motivated by the goal to accelerate particles with the large fields generated by focused laser light. The aim of most novel laser-based particle acceleration schemes is to transfer the energy from electromagnetic radiation to particle beams on short

Optics EXPRESS

time and length scales. Recently, several schemes have been developed that employ different strategies to reach efficient acceleration of particles via the interaction with light. In the laser-wakefield acceleration scheme [1,2], high-energy femtosecond laser pulses are used to drive a wake wave in a plasma. Particles can be trapped in such a wave and accelerated to energies of several GeV [3–5]. Another example is the so-called inverse free-electron laser [6,7], where the electrons are accelerated via interaction with laser fields inside the periodic magnetic fields of an undulator. Furthermore, laser acceleration is possible using high-intensity laser pulses focused into a near-critical plasma [8].

The technique described in this paper falls into the family of techniques called dielectric laser acceleration (DLA) [9–12]. DLA employs optical near-fields in the form of evanescent waves excited at various types of periodic dielectric nanostructures. However, not only the energy modulation but also the ultrafast control of freely propagating electrons via their interaction with optical near-fields of short light pulses brings new applications. It has recently led to the development of novel techniques of time-resolved electron imaging with enhanced contrast [13–15], sub-optical-cycle manipulation of electrons [11,16,17] and quantum coherence studies of the interaction between free electrons and optical near-fields [18–20], opening the field of free electron quantum optics.

Due to the different dispersion relations of electrons and photons in vacuum, the efficient (first order) interaction of electrons and photons is forbidden. In other words, energy and momentum cannot be conserved at the same time in vacuum for photon absorption or emission by an electron (for details see the Lawson-Woodward theorem [21]).

An efficient interaction between laser light and travelling charged particles can be achieved by slowing down the phase velocity of electromagnetic waves via the presence of matter and match it to the group (propagation) velocity of the particles. Without dispersion, light waves propagate in vacuum at a phase velocity equaling the vacuum speed of light c. However, in optical near-fields generated close to the surface of an object with a refractive index $n>1$, the phase velocity can be reduced below c [22]. In DLA, periodic structures are used to enhance the interaction distance to several hundreds of micrometers [9,10]. Due to the structural periodicity in the electron propagation direction and the side-coupling of the excitation light, the near-fields can be described via spatial Fourier transformation as a series of spatial harmonics propagating with different phase velocities. To attain the synchronous interaction between electrons and the fundamental harmonic, the periodicity of the structure has to fulfill the synchronicity condition $\beta = \lambda_p / \lambda$, where $\beta = v_e/c$ is the dimensionless electron velocity, λ_p is the nanostructure period and λ is the laser wavelength [23]. When illuminated by pulses at visible to mid-infrared wavelengths, DLA devices need advanced nanofabrication techniques to obtain feature sizes less than 100 nm, with stringent requirements for the fabrication precision.

In this paper we propose and experimentally demonstrate an alternative approach using the interaction of free electrons with an evanescent wave excited on the planar (non-structured) surface of a dielectric material by total internal reflection. A similar idea, using two dielectrics and two driving laser beams, was theoretically proposed in [24]. This approach can be advantageous for the following reasons: i) simpler or no nanofabrication is required, dramatically reducing the complexity of experiments studying electron manipulation by light fields; ii) the laser damage threshold of bulk material with optically polished surfaces is usually higher than the damage threshold of nanofabricated surfaces due to better heat dissipation, the fewer lattice imperfections and impurities produced during the nanofabrication process and the lack of field enhancement at the sub-wavelength features of nanostructured devices; iii) the interaction length can be extended by coupling the light into an optical waveguide; iv) material classes with high laser damage thresholds may be used that can hardly or not at all be nano-structured, such as SiC, Al_2O_3 or CaF_2 [25]; and v) the incident angle of the totally reflected beam can be varied to tune the phase velocity of the evanescent wave.

Optics EXPRESS

In the theory part of this paper we describe the interaction between an evanescent wave and an electron in the classical approximation with electrons as point-like particles. The solution of the equation of motion is derived for electrons synchronously interacting with an evanescent wave propagating along the dielectrics´ surface in the approximation of small relative electron velocity change. In the experimental part we show the results of a proof-of-principle experiment demonstrating the acceleration of electrons by an optical evanescent wave generated at a non-structured surface using a sub-relativistic electron beam.

2. Theory

The geometry of the experiment is shown in Fig. 1(a) together with the longitudinal component of the electric field E_z. The TM polarized plane wave impinges with an angle of incidence θ_i on the planar interface (x-z plane) between a dielectric with refractive index n>1 and vacuum. To excite the evanescent wave via total internal reflection, θ_i must be larger than the critical angle θ_c = arcsin(1/n). By applying Maxwell's equations at the boundary with an incoming plane wave at angular frequency ω and incident electric field amplitude E_i, the electromagnetic fields on the vacuum side (transmitted wave) can be written as [26]:

$$\vec{E}_t(y,z,t) = \mathrm{Re}\left\{ \begin{array}{l} aE_i\left(n\sin\theta_i\vec{e}_y - i\sqrt{n^2\sin^2\theta_i - 1}\vec{e}_z\right)\times \\ \exp\left[-\frac{\omega}{c}\sqrt{n^2\sin^2\theta_i - 1}y + i\left(\frac{\omega}{c}zn\sin\theta_i - \omega t + \varphi_0\right)\right] \end{array}\right\}$$

$$\vec{B}_t(y,z,t) = \mathrm{Re}\left\{-\frac{aE_i}{c}\exp\left[-\frac{\omega}{c}\sqrt{n^2\sin^2\theta_i - 1}y + i\left(\frac{\omega}{c}zn\sin\theta_i - \omega t + \varphi_0\right)\right]\vec{e}_x\right\}, \quad (1)$$

$$a = \frac{2n\cos\theta_i}{\cos\theta_i - in\sqrt{n^2\sin^2\theta_i - 1}}$$

where φ_0 is the initial phase of the incident plane wave and $\vec{e}_x, \vec{e}_y, \vec{e}_z$ are unit vectors along the Cartesian axes. From Eq. (1) we can infer the most important properties of the evanescent wave excited at the interface: i) Its phase front is perpendicular to the interface while the intensity front is parallel to the interface. ii) The field amplitude decays exponentially in the y direction with a decay length $\Gamma = c/(\omega\sqrt{n^2\sin^2\theta_i - 1})$. iii) The phase velocity of the evanescent wave $v_{ph} = c/(n\sin\theta_i)$ can be synchronized with the group velocity of an electron (or any charged particle) $v_e = \beta$c moving along the surface. In this case, the decay length $\Gamma = \gamma\beta\lambda/2\pi$ is only a function of the electron velocity and the light wavelength. Further, it matches the field decay length of the first spatial harmonic of the near-field mode of periodic nanostructures [23]. Using high-refractive index materials, the wave can be slowed down to ~0.3c and therefore interact synchronously even with sub-relativistic electrons at energies of only several tens of keV.

Because the amplitude of the electron energy modulation (hundreds of eV) is much higher than the infrared photon energy used in the experiment (0.64 eV), the description of the interaction falls beyond perturbation theory. It can rather be described classically by solving the equation of motion with the Lorentz force for an individual point-like particle:

$$\frac{d}{dt}(\gamma m_e\vec{v}_e) = q_e\left(\vec{E} + \vec{v}\times\vec{B}\right). \quad (2)$$

Here m_e and q_e are the electron's rest mass and charge, respectively, and $\vec{E}$ and $\vec{B}$ are the electric and magnetic fields from Eq. (1). This equation has an analytical solution when we

Optics EXPRESS

approximate that the change of the electron's velocity is small, $\Delta\vec{v}_e \ll \vec{v}_e$, during the interaction ($v_e \gg v_{ph}$). Such an approximation is valid either for the interaction over short distances and times or for relativistic electrons with $v_e \approx c$ ($\beta = 1$). In this case, Eq. (2) can be directly integrated with the fields from Eq. (1). The final electron's kinetic energy as a function of its initial distance from the surface y and the phase of the evanescent wave φ can be written as:

$$E_k(\varphi) = E_{k0} + qv_e \int_{-\infty}^{\infty} E_i(t)dt \,\mathrm{Re}\left\{ia\sqrt{\beta^{-2}-1}\exp(i\varphi)\right\}\exp\left(-\frac{\omega}{c}\sqrt{\beta^{-2}-1}y\right), \quad (3)$$

where $E_i(t)$ describes the evolution of the incident electric field amplitude as a function of time for a laser pulse (assuming that the envelope varies slowly as compared to the carrier period). For DLA applications, an important quantity is the maximum acceleration factor $F_{max} = E_z(y=0)/E_i = |a|\sqrt{\beta^{-2}-1}$, which describes the ratio between the longitudinal component of electric field of the evanescent wave at the surface and the incident field amplitude. $F(\beta)$ is plotted for different dielectric materials in Fig. 1(b). For high-refractive index materials we see that the acceleration factor can be as high as 1.8. However, F_{max} is defined here using the incident field strength inside the material. If we take into account the factor $\sqrt{n}$, which results from the ratio between the field amplitude of the driving laser field in vacuum and that in the material (coupling of the laser), we obtain $F_{max} \sim 1$. The minimum electron velocity for the interaction is limited to $\beta_{min} = 1/n$ for the situation where the incident plane wave is propagating inside the material along the z axis. In this case the longitudinal component of the field vanishes and no evanescent wave is excited. The acceleration factor also determines the maximum acceleration gradient (the kinetic energy gain per unit distance) which can be reached as $G_{max} = \mathrm{d}E_k/\mathrm{d}s$. Its value in the approximation of small relative velocity change is:

$$G_{max} = qE_{imax}|a|\sqrt{\beta^{-2}-1} = qE_{imax}F, \quad (4)$$

where E_{imax} is the peak incident field amplitude. For sub-relativistic electrons interacting with realistic peak fields below the material damage threshold (~GV/m), the approximation of the small velocity change is valid only for interaction lengths smaller than a few micrometers. The strong modulation of the electrons´ velocity leads to a violation of the synchronicity condition and subsequent dephasing of electrons and the evanescent wave. This effect was already theoretically described for grating-based DLA experiments [23] where the dephasing length was defined as the distance after which the electrons with maximum energy gain slip over a phase difference of $\pi/2$ with respect to the synchronous mode. The dephasing length for an electron interacting with an evanescent wave can be written as [23]:

$$z_{deph} = \left[\frac{\pi\beta c E_k\left(\frac{E_k}{m_0c^2}+1\right)\left(\frac{E_k}{m_0c^2}+2\right)}{2\omega G_{max}}\right]^{1/2}. \quad (5)$$

To investigate the dephasing effect in a realistic way we performed numerical simulations using a 4th order Runge-Kutta integration of Eq. (2). For the sub-relativistic electron beam with $\beta = 0.32$ used in our experiments, dephasing limits the maximum achievable energy gain to ~1-3 keV depending on the applied field strength and interaction distance.

Optics EXPRESS

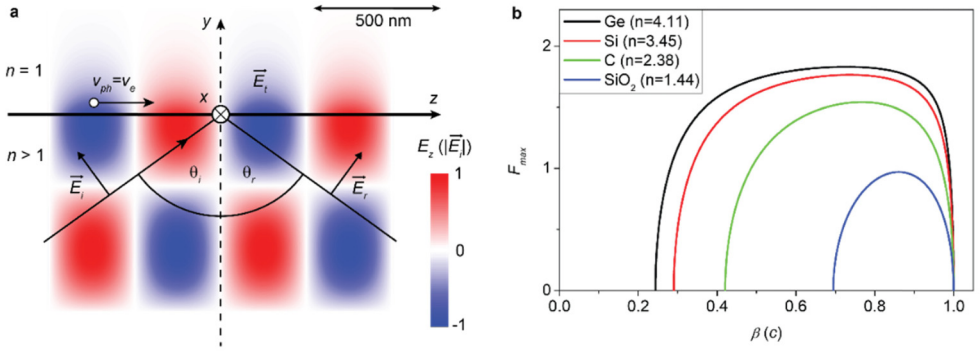

Fig. 1. a) Total internal reflection at the surface of the dielectric, which extends from negative y to $y = 0$. Electrons propagate from left to right along the surface with group velocity v_e and interact with the evanescent wave propagating with phase velocity v_{ph}. Color bar: temporal snapshot of the longitudinal component of the electric field of light E_z calculated at the interface between silicon ($n = 3.4$) and vacuum for $\lambda_0 = 2$ µm, $\theta_i = 60°$. b) Dependence of the maximum acceleration factor $F_{max} = E_z(y = 0)/E_i$ on the electron velocity $\beta = v_e/c$ for various materials (germanium, silicon, diamond and fused silica) whose index of refraction is given in the inset.

3. Experimental setup

To measure the energy spectrum of electrons after the interaction with the optical evanescent wave we use the setup described in detail in [27]. A scanning electron microscope (Hitachi S-Series) serves as a source of electrons with tunable energy in the range of 3-30 keV. The beam is focused to a spot size of $w_e = 70$ nm ($1/e^2$ radius, approx. Gaussian transverse spatial mode) and sent along the surface of various dielectrics. Due to the rather low electron velocity of $\beta = v_e/c = 0.32$ used in the experiment, corresponding to an initial kinetic energy of $E_{k,in} = 28.4$ keV, the high refractive index materials germanium ($n = 4.11$ [28]) and silicon ($n = 3.45$ [28]) are employed in this proof-of-principle experiment to match the phase velocity of the evanescent wave to β. With band gaps of 0.67 eV and 1.12 eV, respectively, both materials are transparent for the laser pulses used in this study. We excite the evanescent wave with laser pulses derived from a thulium-doped femtosecond fiber laser. The pulse duration equals $\tau_{FWHM} = 600$ fs at a center wavelength of $\lambda = 1.93$ µm, corresponding to a mean photon energy of $\hbar\omega = 0.64$ eV. The laser repetition rate is $f_{rep} = 1$ MHz. The pulses are amplified in a rod-type thulium-doped fiber amplifier, which yields a maximum average power of 30 W and a maximum pulse energy of $E_p = 30$ µJ. During the experiments, we limit the average power to 0.5 W to prevent sample damage. The laser pulses are focused onto the DLA structures to a spot with a $1/e^2$ intensity radius of $w_l = 16$ µm (only one half of the transverse laser intensity profile is used in the experiments due to clipping of the laser beam at the edge of the sample for alignment reasons). The interaction length is further increased due to the angle of refraction to $w_{int} = 23.5$ µm [23]. After the interaction with the optical evanescent wave, the electrons are spectrally filtered by a retarding-field spectrometer and detected by a microchannel-plate detector [27].

The evanescent wave is excited in two different geometries (see Fig. 2). In both cases, the incident laser and electron beams are perpendicular with respect to each other. The nonzero angle of incidence of the laser beam at the dielectric interface along the electron beam trajectory is achieved by single or double refraction on planar surface. For the germanium sample, the high value of the refractive index allows us to directly reach the total internal reflection condition by a single refraction of the incident laser beam. For this purpose, a prism with an opening angle of $\alpha = 60°$ is used. In Fig. 2(a) we plot the snapshot of the spatial distribution of E_z relative to the incident laser field amplitude $E_{z,inc}$ obtained using a numerical finite-difference time-domain modeling (FDTD) [29]. Due to the refraction angle on the first

Optics EXPRESS

boundary and the high refractive index, the incident field inside the structure exciting the evanescent wave is smaller compared to the incident field of the laser pulses in vacuum, leading to a maximum acceleration factor of F_{max}~0.5.

In the case of silicon, double refraction is necessary to reach the synchronicity condition at the surface perpendicular to the incident laser wavevector (see Fig. 2(b)). We have therefore fabricated a silicon microstructure with the help of electron beam lithography and reactive ion etching that allows us to reach the required angle of incidence to match the phase velocity of the evanescent wave to the propagating electrons´ velocity. A scanning electron microscope (SEM) image of the silicon sample with the laser beam path is shown in Fig. 2 (b).

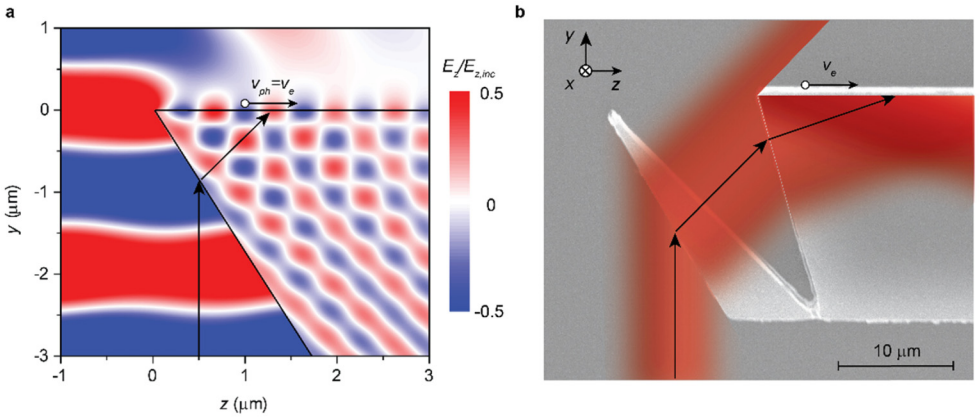

Fig. 2. a) Excitation of an optical evanescent wave by single refraction using a germanium prism. Colorscale: electric field component E_z calculated numerically using FDTD technique. b) SEM image of the silicon microstructure which serves for the excitation of an optical evanescent wave using two subsequent refractions of the laser beam (beam path in the ray optics approximation indicated by the red overlay and the black arrows).

4. Results and discussion

The measured spectra of electrons accelerated by the interaction with the evanescent wave are shown in Fig. 3. In addition, we show for comparison the results of numerical simulations. The maximum observed energy gains for germanium (red squares) and silicon (black circles) samples were 800 eV and 300 eV, respectively. The coupling efficiency of the incident laser field to the evanescent wave varies due to the difference in refractive index (see Fig. 1(b)) and also due to different coupling schemes (Fig. 2). In the case of germanium, the maximum energy modulation is already close to the dephasing limit. The low maximum energy gain obtained with the silicon structures indicates a poor quality of the silicon surface (see Fig. 2(b)) in comparison with the germanium surface polished to optical quality. Due to the deep etching necessary for reaching the desired height of the silicon structures, the surface roughness is ~100 nm, which is comparable to the spatial decay length of the evanescent wave.

Optics EXPRESS

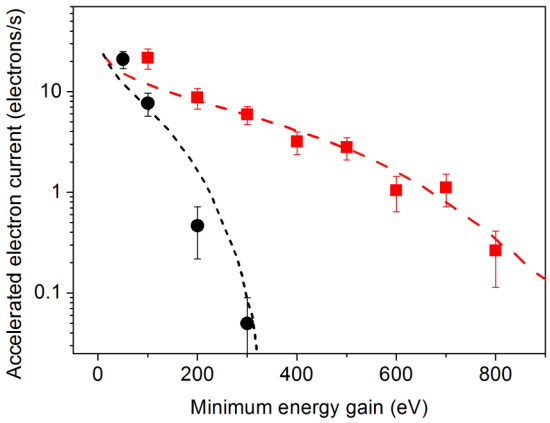

Fig. 3. Measured accelerated electron current as a function of the minimum energy gain for Ge (red squares) and Si (black circles). Independent numerical simulation results are shown as dashed curves. With an initial electron kinetic of $E_{k,in}$ = 28.4 keV, the maximum energy gain equals 800 eV for germanium and 300 eV for silicon. The acceleration is stronger for germanium because of its higher refractive index and because of the coupling geometry with only single refraction of the driving beam.

The numerical simulation results (dashed curves in Fig. 3) are obtained using the electron and laser beam parameters given in the experimental section above. The distance between the center of the electron beam and the sample surface d was used as a fitting parameter. The experimental spectrum was obtained with the electron beam as close as possible to the surface. According to fit results, this corresponds to d = 200 nm, which is almost twice the transverse decay length of the field Γ = 105 nm. The reason why the DC electron beam cannot reach closer to the sample surface is likely the charging of the surface by electrons colliding with it. Despite the fact that a doped silicon is used in the experiments, the charging of surfaces of both germanium and silicon samples appear similar as revealed from the SEM images of the structure shortly after switching from the point mode (electron beam at a constant position close to the surface) to the scanning mode (imaging by scanning the electron beam along the sample) of the SEM. This leads to a repulsion force acting on the electron beam. Also the surface roughness of the surface can play a role here. These effects limit the maximum acceleration gradient to G_{max} = 19 ± 2 MeV/m, which is much lower than the theoretically expected value of G_{max} = 500 MeV/m for the electron at y = 0 on a perfectly flat surface. This value is comparable with 25 MeV/m obtained in the proof-of-principle experiment with sub-relativistic electrons employing the inverse Smith-Purcell effect at a single nanograting [10]. The electron count rate in the experiment is limited by the interaction of a continuous electron beam with the pulsed laser. The average current of interacting electrons is given by the electron probe current (I_p = 3 pA) and the laser duty-cycle ($D = 6 \times 10^{-7}$) as $I_{int} = I_p D \approx 11$ e$^-$/s. With a laser-triggered electron source, this can be many orders of magnitude larger in the future.

To confirm experimentally that the energy modulation is caused exclusively by the interaction with the evanescent wave, the spatial profile of the synchronous fields is characterized by measuring the accelerated electrons´ spectra as a function of the distance from the germanium sample surface. The results are shown in Fig. 4. The measured transverse field decay length $\Gamma = 90 \pm 10$ nm obtained by fitting the dependence of the current of electrons with an energy gain higher than 120 eV as a function of d (see the inset of Fig. 4). It agrees with the theoretical value of Γ = 105 nm. The other possible contributions to the observed energy gain of the electrons are the ponderomotive interaction arising from the gradient of the light intensity [30] at the sample edge and a longitudinal kick due to a high-density cloud of electrons photo-emitted from the structure by the laser pulse. However, both

Optics EXPRESS

effects are excluded by the observed exponential transverse decay of the accelerating field. Moreover, the ponderomotive energy (the average kinetic energy of the electron during quiver motion in the laser field) $U_p = e^2E^2/(4m_e\omega^2) = 0.2\,\text{eV}$ is small compared to the observed energy gain of few hundreds eV.

The short transverse decay length has further consequences for the requirements of the electron beam transverse size and emittance. To ensure 10% relative uniformity of the accelerating field along the transverse profile of the beam, the condition w_e<10 nm has to be fulfilled along the interaction length. However, in more advanced structures with a cosh-like transverse spatial mode [24], the homogeneity of the field in the center of the gap allows to increase w_e approx. by a factor of 10. This small transverse acceptance of the accelerating structure also limits the peak current of electrons that can interact with the evanescent wave over extended distances due to Coulomb repulsion effects.

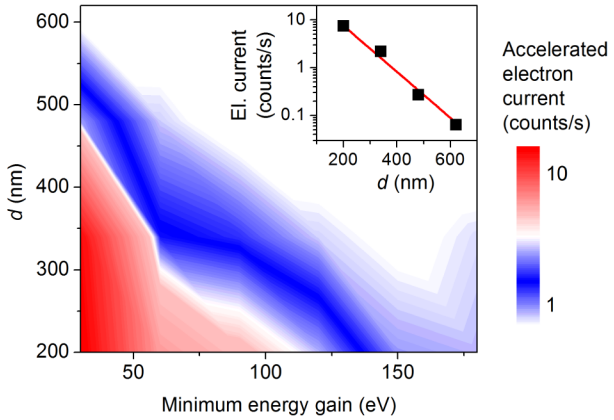

Fig. 4. Accelerated electron current (color scale) plotted on a log scale as a function of minimum energy gain and distance d between the electron beam center and the germanium sample surface. Inset: Dependence of the current of electrons with energy gain higher than 120 eV on the distance d (squares) plotted on log scale. The full red line shows the exponential fit to the data with decay length of $\Gamma = 90 \pm 10$ nm, in fair agreement with the theoretical value of 105 nm. We conclude that the electrons are indeed accelerated with the evanescent surface field.

The modulation of the electrons´ kinetic energy can serve for temporal gating of ultrashort sub-optical cycle electron bunches [16]. For this purpose, an energy analyzer is required to filter the electrons that obtain an energy modulation during the interaction. The measured energy change then serves as a monitor of the spatio-temporal overlap between electrons and the laser pulse [11,16]. However, the transverse field component of the evanescent wave (see Eq. (1)) leads to a deflection of electrons in the y direction parallel to the laser beam propagation. This effect was already demonstrated for the interaction of electrons with optical near-fields of periodic nanostructures [12,31]. Spatial separation of the deflected and non-deflected electrons after the interaction does not require a spectrometer and only a simple spatial mask or adjustable knife edge in front of the electron detector is required to filter the interacting electrons [16].

Also the transverse electron momentum in the x direction perpendicular to both laser and electron beams can be controlled by the interaction with the evanescent wave. At periodic nanostructures, the transverse force component can be generated by tilting the structure with respect to the electron beam direction [16,32]. For the case of our experiment where the electrons propagate in the plane of incidence of the totally internally reflected wave (Fig. 1), the x-component of the force vanishes. However, by tilting the plane of incidence of the laser wave with respect to the electron beam propagation direction at an angle α, $F_x \neq 0$. The force

Optics EXPRESS

acting on an electron can be calculated from (1) and (2) by standard rotation transformations as:

$$\vec{F} = q\,\mathrm{Re}\left[-iA\sqrt{\beta_{defl}^{-2}-1}\sin\alpha\vec{e}_x + \left(\beta_{defl}^{-1}-\beta_{defl}\right)A\vec{e}_y - iA\sqrt{\beta_{defl}^{-2}-1}\cos\alpha\vec{e}_z\right]$$
$$A = aE_i\exp\left[-\frac{\omega}{c}\sqrt{\beta_{defl}^{-2}-1}\,y + i\left(\frac{\omega}{c}zn\sin\theta_i - \omega t + \varphi_0\right)\right], \quad (6)$$

where $\beta_{defl} = \beta\cos\alpha$. Thus by simple modification of the experiment, the optical field-based control over the electron momentum can be extended also to the second transverse direction. We note that in this case the phase velocity of the evanescent wave needs to be further slowed down in comparison with the case $\alpha = 0$. The deflection of the sub-relativistic electron beam used in this study would thus require a material with an even higher refractive index than germanium, or an electron beam with a velocity β>0.5.

5. Conclusions

We have theoretically and experimentally demonstrated the inelastic interaction between an optical evanescent wave excited by total internal reflection on a planar vacuum-dielectric interface with a beam of sub-relativistic freely propagating electrons. We have shown that an energy gain as high as 800 eV can be reached. This is achieved by an evanescent wave with a phase velocity that is synchronized with the electron propagation velocity by using high refractive index materials. The observed acceleration gradient is G_{max} = 19 ± 2 MeV/m, which is likely limited by charging of the structure and its surface quality. For optimal surface with roughness of 1-10 nm and wide band gap dielectrics such as CaF_2, values as high as G_{max}>10 GeV/m are expected due to the high laser damage threshold of these materials [25]. The future use of this effect is not limited to evanescent waves excited by total internal reflection. The modes coupled to optical fibers and planar waveguides decay exponentially with the distance from the core forming an evanescent optical wave. If the cladding is replaced by vacuum, such as in silicon-on-insulator waveguides, an electron beam can interact with an evanescent field of a coupled mode over longer distances [33]. This would lead to a decrease of the optical power necessary to transfer the same amount of energy to the electrons. Furthermore, this interaction can find application in ultrafast optical gating of electron beams as well as in free space electron quantum optics experiments.

Funding

Gordon and Betty Moore Foundation (Accelerator on a Chip International Program - ACHIP, GBMF4744); European Research Council (Near Field Atto); Bundesministerium für Bildung und Forschung (05K16WEC).